Polaron and molecular states of a spin-orbit coupled impurity in a spinless Fermi sea

Hong-Hao Yin(尹洪浩), Tian-Yang Xie(谢天扬), An-Chun Ji(纪安春), and Qing Sun(孙青)
Citation: Chin. Phys. B, 2021, 30 (**10**): 106702. DOI: 10.1088/1674-1056/ac1b85
Journal homepage: http://cpb.iphy.ac.cn; http://iopscience.iop.org/cpb

What follows is a list of articles you may be interested in

Spinor *F*= 1 Bose-Einstein condensates loaded in two types of radially-periodic potentials with spin-orbit coupling

Ji-Guo Wang(王继国), Yue-Qing Li(李月晴), Han-Zhao Tang(唐翰昭), and Ya-Fei Song(宋亚飞)
Chin. Phys. B, 2021, 30 (**10**): 106701. DOI: 10.1088/1674-1056/ac1411

Bose-Einstein condensates under a non-Hermitian spin-orbit coupling

Hao-Wei Li(李浩伟) and Jia-Zheng Sun(孙佳政)
Chin. Phys. B, 2021, 30 (**6**): 066702. DOI: 10.1088/1674-1056/abd7e4

Ground-state phases and spin textures of spin–orbit-coupled dipolar Bose–Einstein condensates in a rotating toroidal trap

Qing-Bo Wang(王庆波), Hui Yang(杨慧), Ning Su(苏宁), and Ling-Hua Wen(文灵华)
Chin. Phys. B, 2020, 29 (**11**): 116701. DOI: 10.1088/1674-1056/abbbe8

Spatiotemporal Bloch states of a spin-orbit coupled Bose-Einstein condensate in an optical lattice

Ya-Wen Wei(魏娅雯), Chao Kong(孔超), Wen-Hua Hai(海文华)
Chin. Phys. B, 2019, 28 (**5**): 056701. DOI: 10.1088/1674-1056/28/5/056701

Phase diagram and collective modes in Rashba spin–orbit coupled BEC: Effect of in-plane magnetic field

Dong Dong, Zou Xu-Bo, Guo Guang-Can
Chin. Phys. B, 2015, 24 (**7**): 076701. DOI: 10.1088/1674-1056/24/7/076701

Polaron and molecular states of a spin–orbit coupled impurity in a spinless Fermi sea*

Hong-Hao Yin(尹洪浩), Tian-Yang Xie(谢天扬), An-Chun Ji(纪安春), and Qing Sun(孙青)†

Department of Physics, Capital Normal University, Beijing 100048, *China*

(Received 30 April 2021; revised manuscript received 21 July 2021; accepted manuscript online 7 August 2021)

We investigate the polaron and molecular states of a fermionic atom with one-dimensional spin–orbit coupling (SOC) coupled to a three-dimensional spinless Fermi sea. Because of the interplay among the SOC, Raman coupling and spin-selected interatomic interactions, the polaron state induced by the spin–orbit coupled impurity exhibits quite unique features. We find that the energy dispersion of the polaron generally has a double-minimum structure, which results in a finite center-of-mass (c.m.) momentum in the ground state, different from the zero-momentum polarons where SOC are introduced into the majority atoms. By further tuning the parameters such as the atomic interaction strength, a discontinuous transition between the polarons with different c.m. momenta may occur, signaled by the singular behavior of the quasiparticle residue and effective mass of the polaron. Meanwhile, the molecular state as well as the polaron-to-molecule transition is also strongly affected by the Raman coupling and the effective Zeeman field, which are introduced by the lasers generating SOC on the impurity atom. We also discuss the effects of a more general spin-dependent interaction and mass ratio. These results would be beneficial for the study of impurity physics brought by SOC.

Keywords: spin–orbit coupling, polaron, Fermi gas

PACS: 67.85.Lm, 03.75.Ss, 05.30.Fk **DOI:** 10.1088/1674-1056/ac1b85

1. Introduction

Coupling a mobile impurity to a many-body environment in a controllable way provides a handleable method to study the unique physics of emergent quasiparicles, *e.g.*, the polarons in diverse systems.[1–4] Among them the ultracold gases, being an ideal platform of high tunability and cleanness, have been utilized to explore the intriguing impurity physics[5–9] and many important advances have been achieved.[10–12] For examples, the realizations of Fermi polarons in spin-polarized Fermi gases,[13–35] the polarons in Bose–Einstein condensates (BEC),[36–40] and the polaron-to-molecule transitions,[41–44] which are usually surveyed by varying the interaction strength between the impurity atom and the surrounding atoms via Feshbach resonance.[45]

Recent years, the implementation of spin–orbit coupling (SOC) in ultracold gases[46–50] stimulates tremendous researches on the nontrivial effects brought by SOC,[51–60] which also enriches the content of the impurity physics in cold atom systems.[61–64] In general, SOC mixes different spin components of the atom and changes the single-particle dispersion dramatically, which may lead to the enhanced low-energy density of state and possible single-particle ground-state degeneracy[46,60] responsible for the many-body behaviors of the underlying systems. A series of Fulde–Ferrell–Larkin–Ovchinnikov-like molecule states are predicted in different impurity models with SOC.[61,62] Nevertheless, previous works focus on the cases that the SOCs are mainly introduced to the majority atoms of the environment.[62,63] Due to the heating problem caused by the Raman lasers to generate SOCs in current experiments,[55] it would be difficult to reach the degenerate regime of the majority atoms especially for the Fermi gas.

In this paper, we consider a different situation that a one-dimensional (1D) SOC is introduced solely to the impurity atom, which is immersed in a three-dimensional (3D) spinless Fermi sea formed by the majority atoms. One of the advantages of this configuration is that the majority atoms are not affected directly by the Raman lasers avoiding heating, and thus facilitates the investigation and manipulation of the impurity states by SOC. To be specific, in this system, we find that SOC can strongly affect the polaron state via the impurity atom, with the ground state always carrying a finite c.m. momentum. Due to the SOC induced double-minimal structure of the energy spectrum, a first-order transition may occur between two polaron states with different center-of-mass (c.m.) momenta, in contrast to previous works where a zero-momentum polaron is considered.[59–61] Meanwhile, the molecular state is also changed by the SOC, giving rise to a unique polaron-to-molecule transition driven by the Raman coupling. The quasiparticle residue and the effective mass of the polaron, as well as the mass ratio effect are also discussed. Our results suggest a new way to study the impurity physics brought by SOC.

The paper is organized as follows: In Section 2, we give

*Project supported by the National Natural Science Foundation of China (Grant No. 11875195) and the Foundation of Beijing Education Committees (Grant Nos. CIT&TCD201804074 and KZ201810028043).

†Corresponding author. E-mail: sunqing@cnu.edu.cn

the Hamiltonian to describe a spin–orbit coupled impurity atom interacting with a spinless Fermi sea. In Section 3, we analyze the unique properties of the polaron state, including the energy dispersion, the ground-state momentum, the quasiparticle residue, and the effective mass. Moreover, the ground-state transition of the polaron with different c.m. momenta is also discussed. In Section 4, we further present the results of the molecular state and the polaron-to-molecule transition. Finally, we discuss the effects of a more general spin-dependent interaction and mass ratio and conclude in Section 5.

2. The model

We consider a spinful fermionic (impurity) atom of mass $m_{\rm a}$ immersed in a spinless 3D Fermi sea of mass $m_{\rm b}$. A one-dimensional (1D) SOC is introduced into the two spin states (labeled as $\sigma=\uparrow,\downarrow$) of the impurity by a pair of Raman lasers[46] or recoil-dressed photons.[58] In the momentum space, the total Hamiltonian of the system takes the form of (we set $\hbar=1$)

$$\begin{aligned}\hat{H}=&\sum_{\boldsymbol{k}}\left[\sum_{\sigma}\frac{(\boldsymbol{k}+\sigma\boldsymbol{k}_0)^2}{2m_{\rm a}}\hat{a}^{\dagger}_{\boldsymbol{k}\sigma}\hat{a}_{\boldsymbol{k}\sigma}+\frac{\delta}{2}\left(\hat{a}^{\dagger}_{\boldsymbol{k}\uparrow}\hat{a}_{\boldsymbol{k}\uparrow}-\hat{a}^{\dagger}_{\boldsymbol{k}\downarrow}\hat{a}_{\boldsymbol{k}\downarrow}\right)\right.\\&\left.+\frac{\Omega}{2}\left(\hat{a}^{\dagger}_{\boldsymbol{k}\uparrow}\hat{a}_{\boldsymbol{k}\downarrow}+{\rm H.c.}\right)\right]+\sum_{\boldsymbol{k}}\frac{\boldsymbol{k}^2}{2m_{\rm b}}\hat{b}^{\dagger}_{\boldsymbol{k}}\hat{b}_{\boldsymbol{k}}\\&+\frac{g_\sigma}{V}\sum_{\boldsymbol{k}\boldsymbol{k}'\boldsymbol{q},\sigma}\hat{a}^{\dagger}_{\boldsymbol{k}\sigma}\hat{b}^{\dagger}_{\boldsymbol{q}-\boldsymbol{k}}\hat{b}_{\boldsymbol{q}-\boldsymbol{k}'}\hat{a}_{\boldsymbol{k}'\sigma}.\end{aligned}\tag{1}$$

Here, $\hat{a}_{\boldsymbol{k}\sigma}$ and $\hat{b}_{\boldsymbol{k}}$ are the annihilation operators of the impurity atom with spin σ and the majority atoms forming the Fermi sea, respectively. $2\boldsymbol{k}_0$ is the momentum transfer characterizing the strength of SOC, and δ and Ω denote the effective Zeeman splitting (two-photon detuning) and spin flipping (Raman coupling) between the two spin states of the impurity, which can be tuned in experiment.[46,47] g_σ (<0) describes the strength of the contact attraction between the impurity atom of spin σ and the majority atoms, while the interaction between impurity atoms is absent in the single impurity limit. In the following, we first consider a spin-selected interaction by assuming $g_\uparrow\equiv g$ and $g_\downarrow=0$, which can be readily achieved via Feshbach resonance.[45] A more general situation with spin-dependent $g_\downarrow\neq 0$ is discussed later, where the main physics obtained at $g_\downarrow=0$ is not changed significantly up to a considerable $g_\downarrow$. In 3D case, the bare interaction g is renormalized as[65]

$$\frac{1}{g}=-\frac{2\mu}{V}\sum_{\boldsymbol{k}}\frac{1}{k^2}+\frac{\mu}{2\pi a_{\rm s}},\tag{2}$$

where $a_{\rm s}$ is the s-wave scattering length, ranged from the BEC side with $a_{\rm s}>0$ to the BCS side with $a_{\rm s}<0$. $\mu=m_{\rm a}m_{\rm b}/(m_{\rm a}+m_{\rm b})$ is the reduced mass and V is the quantized volume.

3. Polaron state

In the limit of single impurity, the free impurity atom is scattered by the atoms in the Fermi sea to form a dressed state — Fermi polaron,[30] which can have a lower energy than the free impurity state and is expected to be the ground state of this system for a weak attractive interaction. Up to a particle-hole fluctuation, the variational wave-function of the polaron with c.m. momentum $\boldsymbol{Q}$ can be constructed as

$$|P\rangle_{\boldsymbol{Q}}=\left(\sum_{\sigma}\phi_\sigma\hat{a}^{\dagger}_{\boldsymbol{Q}\sigma}+\sum_{\boldsymbol{k}\boldsymbol{q}\sigma}\phi_{\boldsymbol{k}\boldsymbol{q}\sigma}\hat{a}^{\dagger}_{\boldsymbol{Q}+\boldsymbol{q}-\boldsymbol{k}\sigma}\hat{b}^{\dagger}_{\boldsymbol{k}}\hat{b}_{\boldsymbol{q}}\right)|FS\rangle_N,\tag{3}$$

where ϕ_σ and $\phi_{\boldsymbol{k}\boldsymbol{q}\sigma}$ are the amplitudes of a bare impurity of spin σ and that dressed by a particle–hole excitation, respectively. In Eq. (3), we have included both spin states of the impurity atom, which are mixed due to the introducing of 1D SOC.[62] The summation of momentum is limited to $q<k_{\rm F}$ (hole) and $k>k_{\rm F}$ (particle) with $k_{\rm F}$ being the Fermi momentum of the Fermi sea $|FS\rangle_N$ formed by N atoms. Minimizing $\langle P|\hat{H}-E_{\rm P}|P\rangle_{\boldsymbol{Q}}$ with respect to ϕ_σ and $\phi_{\boldsymbol{k}\boldsymbol{q}\sigma}$, we can obtain the polaron energy $E_{\rm P}$ (relative to the Fermi sea), which is determined by the following equation (see Appendix A for more details):

$$\begin{aligned}&E_{\rm P}-\frac{(\boldsymbol{Q}+\boldsymbol{k}_0)^2}{2m_{\rm a}}-\frac{\delta}{2}-\frac{\Omega^2}{4}\left(E_{\rm P}-\frac{(\boldsymbol{Q}-\boldsymbol{k}_0)^2}{2m_{\rm a}}+\frac{\delta}{2}\right)^{-1}\\&=\frac{1}{V}\sum_{\boldsymbol{q}}\left(\frac{1}{g}-\frac{1}{V}\sum_{\boldsymbol{k}}\chi^{-1}_{\boldsymbol{k}\boldsymbol{q}}\right)^{-1}.\end{aligned}\tag{4}$$

Here

$$\chi_{\boldsymbol{k}\boldsymbol{q}}=E_{\rm P}-\varepsilon^{\uparrow}_{\boldsymbol{k}\boldsymbol{q}}-\frac{\delta}{2}-\frac{\Omega^2}{4}\left(E_{\rm P}-\varepsilon^{\downarrow}_{\boldsymbol{k}\boldsymbol{q}}+\frac{\delta}{2}\right)^{-1},\tag{5}$$

with

$$\varepsilon^{\uparrow/\downarrow}_{\boldsymbol{k}\boldsymbol{q}}=\frac{(\boldsymbol{Q}+\boldsymbol{q}-\boldsymbol{k}\pm\boldsymbol{k}_0)^2}{2m_{\rm a}}+\frac{k^2}{2m_{\rm b}}-\frac{q^2}{2m_{\rm b}}.$$

The left-hand side of Eq. (4) describes the energy correction on $E_{\rm P}$ from SOC while the right-hand side gives the contribution from the interaction. In what follows, we use $k_0=|\boldsymbol{k}_0|$ and the corresponding energy $\varepsilon_0\equiv(k_0^2/2m_{\rm a})$ as the units of momentum and energy, respectively.

Solving Eq. (4) for each $\boldsymbol{Q}$, we can obtain the energy dispersion of the polaron. As shown in Fig. 1(a), a double-minimum structure of the polaron dispersion is found to be along the direction of $\boldsymbol{k}_0$ due to the SOC, and the lower one gives a nonzero ground-state momentum $\boldsymbol{Q}_{\rm min}=Q_{\rm min}\hat{\boldsymbol{k}}_0$ with $\hat{\boldsymbol{k}}_0$ being the unit vector of $\boldsymbol{k}_0$, where the ground-state energy of the polaron is lower than the free impurity state. More interesting, by varying the interaction strength (scattering length $a_{\rm s}$), the minimum with a higher energy may become the lower one, giving rise to a discontinuous change of $\boldsymbol{Q}_{\rm min}$ between the two minima. In Fig. 1(b), we plot the ground-state momentum $Q_{\rm min}$ as a function of interaction strength for different Zeeman

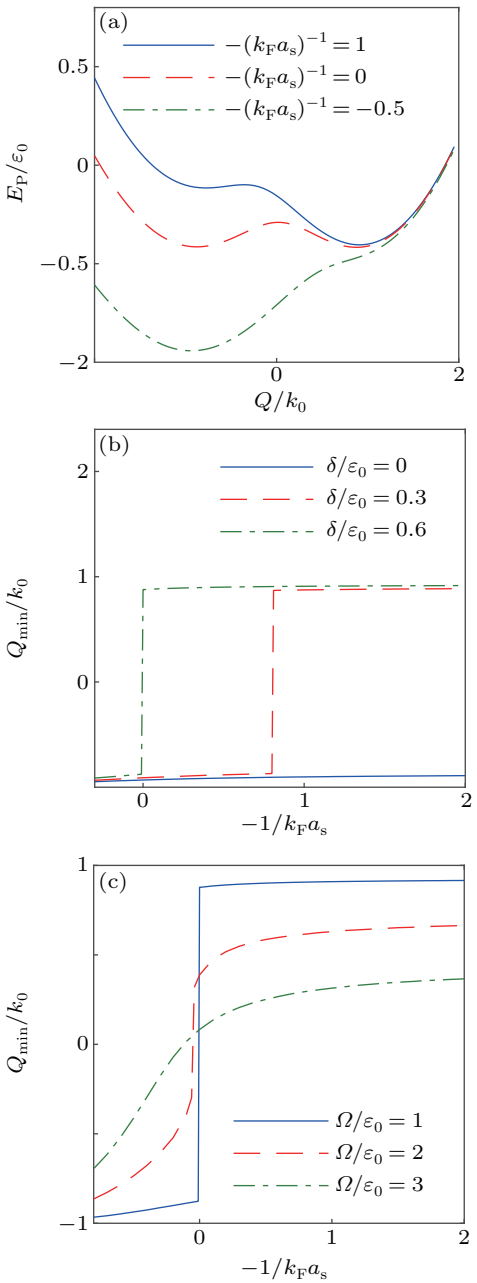

Fig. 1. (a) The polaron energy dispersion E_P with the momentum Q along the direction of SOC for different interaction parameters $-1/(k_Fa_s)$ with $\Omega/\varepsilon_0=1$ and $\delta/\varepsilon_0=0.6$. (b) The ground-state momentum $\boldsymbol{Q}_{min}$ as a function of $-1/(k_Fa_s)$ for different δ with $\Omega/\varepsilon_0=1$. (c) The ground-state momentum $\boldsymbol{Q}_{min}$ as a function of $-1/(k_Fa_s)$ for different Ω with $\delta/\varepsilon_0=0.6$. Here, we have chosen $k_0=k_F$.

splitting δ. One can see that for finite δ, Q_{min} jumps abruptly at a critical interaction strength which increases with δ (the red-dashed and green-dash-dotted lines in Fig. 1(b)). Such discontinuous transition would be smoothened by further increasing the Raman coupling strength Ω, and become a continuous one for $\Omega/\varepsilon_0 \gtrsim 2$ (referred to the green-dash-dotted line in Fig. 1(c)). Physically for $\delta>0$, the (right) minimum with a larger weight of $\downarrow$-component would be the ground state in the weak interaction limit ($a_s<0$), which is weakly dependent on the spin-selected interaction. On the other hand for a sufficiently large interaction strength, the impurity would occupy the (left) minimum with a larger weight of $\uparrow$-component by lowing the interaction energy to compensate the energy cost δ. Notice that for $\delta=0$, such transition is absent and the interaction always favors the minimum state with a larger $\uparrow$-component.

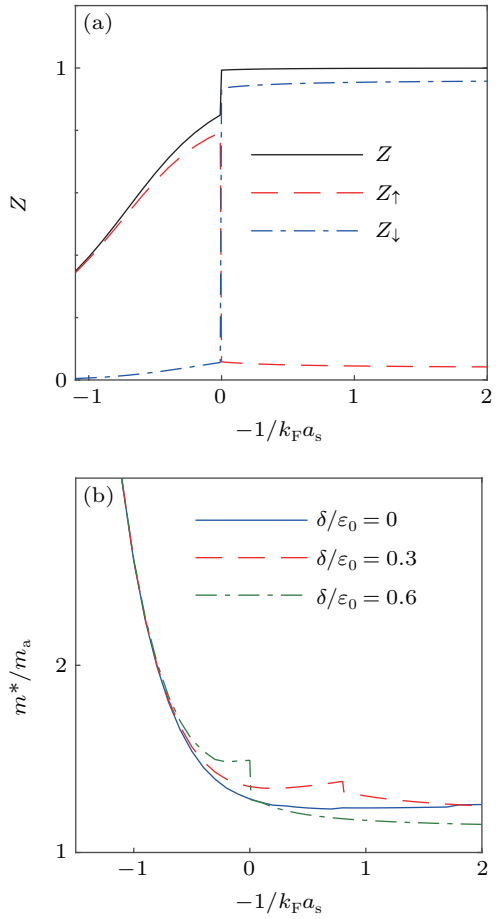

Fig. 2. (a) The quasiparticle residue Z ($Z_{\uparrow/\downarrow}$) as a function of $-1/(k_Fa_s)$ with $\delta/\varepsilon_0=0.6$ and $\Omega/\varepsilon_0=1$. (b) The effective mass m^*/m_a as a function of $-1/(k_Fa_s)$ with other parameters the same in panel (a).

Above picture becomes more transparent when we examine the quasi-particle residue $Z\equiv\sum_\sigma Z_\sigma$ with $Z_\sigma=|\phi_\sigma|^2$, which is given by (see Appendix B for detail)

$$\begin{aligned}\frac{1}{Z} &= 1+\left[1+\frac{\Omega^2}{4}\left(E_P-\varepsilon_{\boldsymbol{Q}}^{\downarrow}+\frac{\delta}{2}\right)^{-2}\right]^{-1}\\ &\times\frac{g^2}{V^2}\sum_{\boldsymbol{kq}}\chi_{\boldsymbol{kq}}^{-2}\left[1+\frac{\Omega^2}{4}\left(E_P-\varepsilon_{\boldsymbol{kq}}^{\downarrow}+\frac{\delta}{2}\right)^{-2}\right]\\ &\times\left(1-\frac{g}{V}\sum_{\boldsymbol{k'}}\chi_{\boldsymbol{k'q}}^{-1}\right)^{-2}.\end{aligned}\tag{6}$$

In Fig. 2(a), we give a typical evolution of Z with the interaction strength for $\Omega/\varepsilon_0=1$ and $\delta/\varepsilon_0=0.6$. Across a critical value, an abrupt jump of Z indicates the discontinuous transition of the ground-state momentum of the polaron. Meanwhile, the state-dependent residue Z_σ also exhibits a sudden change with a larger $Z_\uparrow$ ($Z_\downarrow$) in the regime of relative strong

(weak) interaction. Moreover, due to the spin-selected interaction, $Z \simeq 1$ in the weak interaction regime and decreases quickly in the strong interaction regime ($a_s > 0$) after the transition, where the influence of particle–hole excitation becomes significant. Such unique behaviors of Z can be readily measured in experiment.[19]

Another measurable quantity to characterize the above physics is the effective mass of the polaron, defined as

$$m^* = \frac{1}{2}\left(\frac{\partial^2 E_P}{\partial Q^2}\right)^{-1}_{Q=Q_{min}}. \quad (7)$$

Due to the anisotropy of the energy dispersion, m^* is generally anisotropic and we are interested in the component along $\hat{k}_0$. As shown in Fig. 2(b), we present the relative ratio m^*/m_a as a function of interaction strength. For $\delta > 0$, a similar discontinuous behavior is expected to occur at the critical point. In the limit of $a_s < 0$, the impurity atom is only weakly affected by the interaction and $m^*/m_a \to 1$. While in the BEC regime with $a_s > 0$, the impurity is strongly dressed by the particle–hole excitations, and the effective mass is greatly enhanced towards the instability to the formation of a molecular state discussed in the following.

4. Molecular state and polaron-to-molecule phase transition

When the interaction is strong, a molecular state may appear by tightly binding the impurity atom with one of the majority atoms on top of the Fermi sea. The variational wave function of the molecule with c.m. momentum q can be written as

$$|M\rangle = \sum_{k>k_F,\sigma} \psi_{k\sigma} \hat{a}^\dagger_{q-k\sigma} \hat{b}^\dagger_k |FS\rangle_{N-1}, \quad (8)$$

where $\psi_{k\sigma}$ is the variational amplitude. After a straightforward derivation (see the Appendix C for detail), we obtain the following self-consisted equation for the molecule energy E_M (relative to the Fermi sea):

$$\frac{V}{g} = \sum_k \left[E_M - \frac{|q-k+k_0|^2}{2m_a} - \frac{k^2}{2m_b} - \frac{\delta}{2} - \left(\frac{\Omega}{2}\right)^2 \left(E_M - \frac{|q-k-k_0|^2}{2m_a} - \frac{k^2}{2m_b} + \frac{\delta}{2} \right)^{-1} \right]^{-1}. \quad (9)$$

The ground state of the molecule is determined by further minimizing E_M with respect to q.

Similar to the polaron state, the SOC can also induce a finite c.m. momentum $q_{min} = q_{min}\hat{k}_0$ on the ground state of the molecule. As shown in Fig. 3, in the BEC limit ($a_s \to 0^+$), we have $q_{min}/k_0 \to -1$ irrespective of δ and Ω, and with the increasing of a_s, $|q_{min}|$ first decreases slightly and then increases apparently. Moreover, such dependence of q_{min} on a_s become stronger for a larger δ (Fig. 3(a)) or Ω (Fig. 3(b)). Overall in the presence of the 1D SOC, the molecular state is much less affected than the polaron. This is because that the molecule appears in the strong interaction regime with $a_s > 0$, where the spin-selected interaction binds the impurity in $|\uparrow\rangle$ state with one atom in the Fermi sea tightly. This is in contrast to the polaron state dominant in the weak interaction regime, where the single-particle state of the impurity plays a more important role, and thus more sensitive to the spin splitting δ and spin flipping Ω.

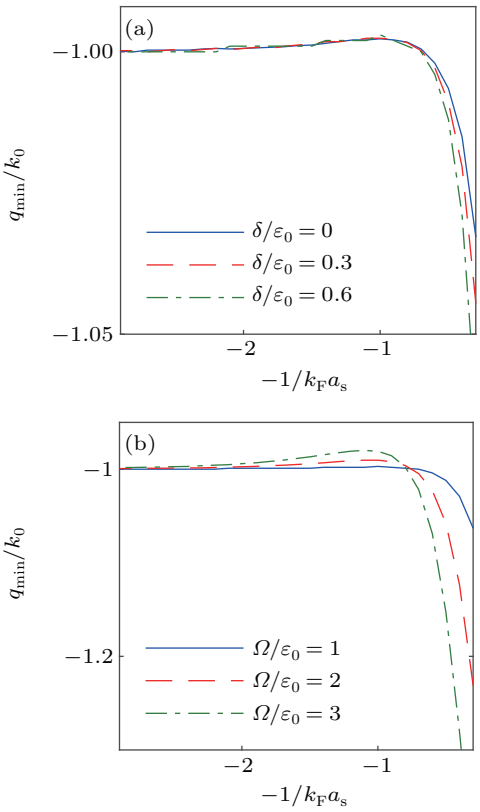

Fig. 3. (a) The molecular ground-state momentum Q_{min} as a function of $-1/(k_F a_s)$ for different Zeeman field δ with $\Omega/\varepsilon_0 = 1$. (b) The molecular ground-state momentum Q_{min} as a function of $-1/(k_F a_s)$ for different Raman coupling strength Ω with $\delta/\varepsilon_0 = 0.6$.

With the polaron and molecular states in hand, we can readily obtain the ground-state phase diagram of the system by comparing the energies of both states. In Fig. 4(a), we show the phase diagram in the $-(1/k_F a_s)$–Ω plane. For $\Omega = 0$, δ gives the same energy shift $\delta/2$ for both E_P and E_M, and hence do not change the critical point. With the increasing of Ω, the phase boundary is pushed into the deep BEC regime gradually, suggesting that the polaron state is more favorable for large Ω. On the other hand, the phase boundary is only weakly dependent on δ (Fig. 4(b)). This can be explained that from Eqs. (4) and (9), the main energy corrections caused by δ are almost the same for E_P and E_M, while Ω corrects E_P more significantly than E_M. Given this, one may address the unique

polaron-to-molecule transition by tuning the Raman coupling (spin flipping) Ω in experiment.

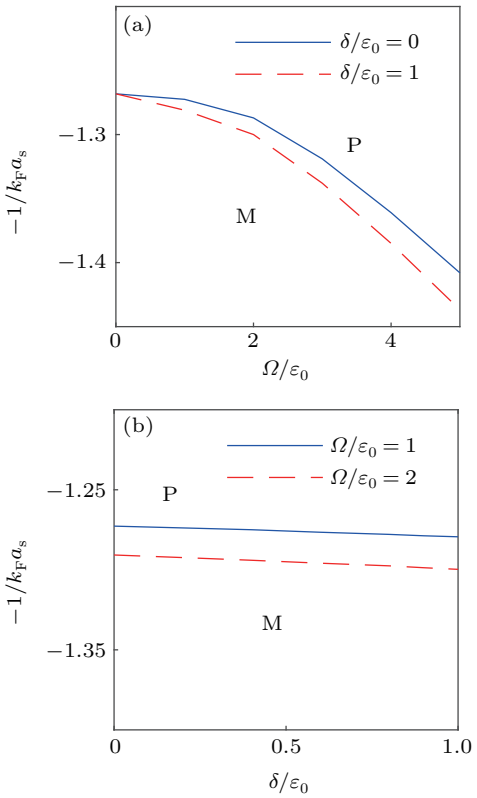

Fig. 4. The ground-state phase diagram (a) in the $-1/(k_F a_s)$–Ω plane for different δ, and (b) in the $-1/(k_F a_s)$–δ plane for different Ω. Here, P and M denote the polaron and molecular states respectively.

5. Discussion and conclusion

Above we have discussed the case of $g_\downarrow = 0$. For a more general spin-dependent interaction with $g_\downarrow \neq 0$, we find that the energy dispersion of the polaron state bears similar double minima structure for different $g_\downarrow/g_\uparrow$, as shown in Fig. 5(a). Correspondingly, the ground-state momentum of the polaron shows a similar behavior as that of $g_\downarrow = 0$ (see Fig. 1(c) and Fig. 5(b)), *i.e.*, it exhibits a discontinuous transition for small $\Omega/\varepsilon_0 = 1$ while varies continuously for large $\Omega/\varepsilon_0 = 3$. The main change is that the transition point moves to the BEC side for a larger $g_\downarrow$, which can be also clearly identified from the effective mass of the polaron shown in Fig. 5(c). These results suggest that a finite $g_\downarrow/g_\uparrow < 1$ would not change the main physics of the polaron state significantly. In Fig. 5(d), we give the phase diagram of the system. With the increasing of $g_\downarrow/g_\uparrow$, the phase boundary is pushed towards the BCS side, indicating that the molecular state is more favorable for a larger $g_\downarrow$.

So far we have focused on the situation that the impurity atom and the majority atoms are of equal mass, which can be achieved by using different hyperfine states of the same species. In experiment, it is also possible to realize a mixture of different species with unequal mass, for example, a mixture of ^{6}Li and ^{40}K with mass ratio $r \equiv m_a/m_b = 6/40$ or $40/6$. As

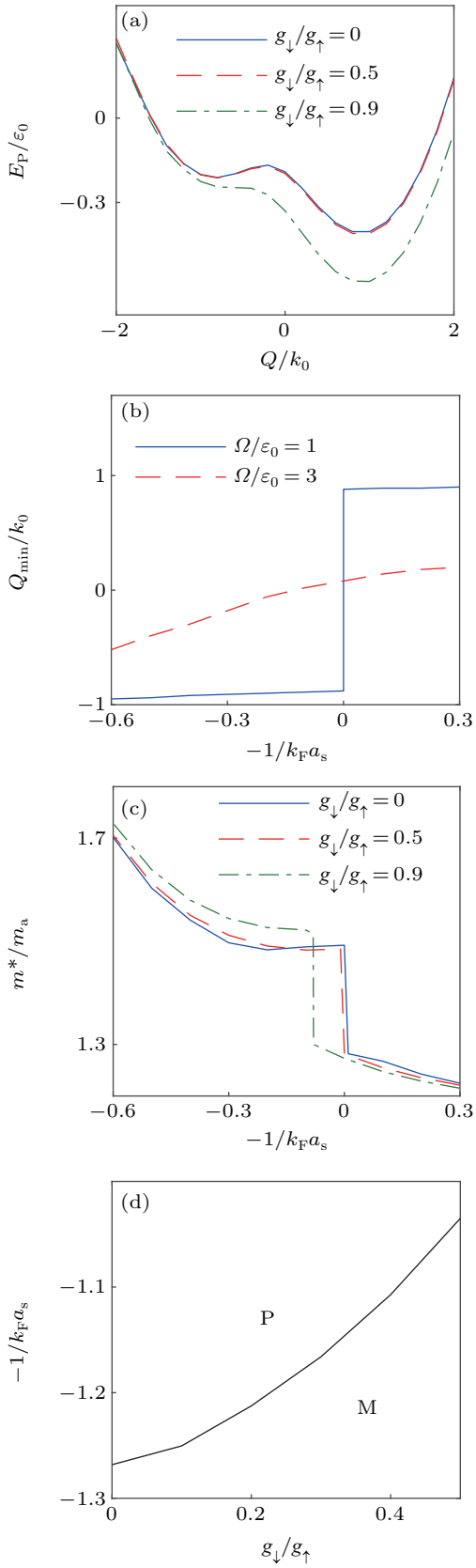

Fig. 5. (a) The energy dispersion E_P of the polaron as a function of Q for different $g_\downarrow/g_\uparrow = 0$ (blue solid), 0.5 (red dashed), and 0.9 (green dash-dotted). (b) The minimal momentum $\boldsymbol{Q}_{min}$ as a function of $-(1/k_F a_s)$ for different Raman coupling strengths $\Omega = 1$ (blue solid) and 3 (red dashed) at $g_\downarrow/g_\uparrow = 0.5$. (c) The effective mass m^* *versus* the interaction parameter for different $g_\downarrow/g_\uparrow = 0$ (blue solid), 0.5 (red dashed), and 0.9 (green dash-dotted). (d) The ground-state phase diagram in the $-(1/k_F a_s)$–$g_\downarrow/g_\uparrow$ plane. Other parameters are $\Omega/\varepsilon_0 = 1$ and $\delta/\varepsilon_0 = 0.6$ if needed.

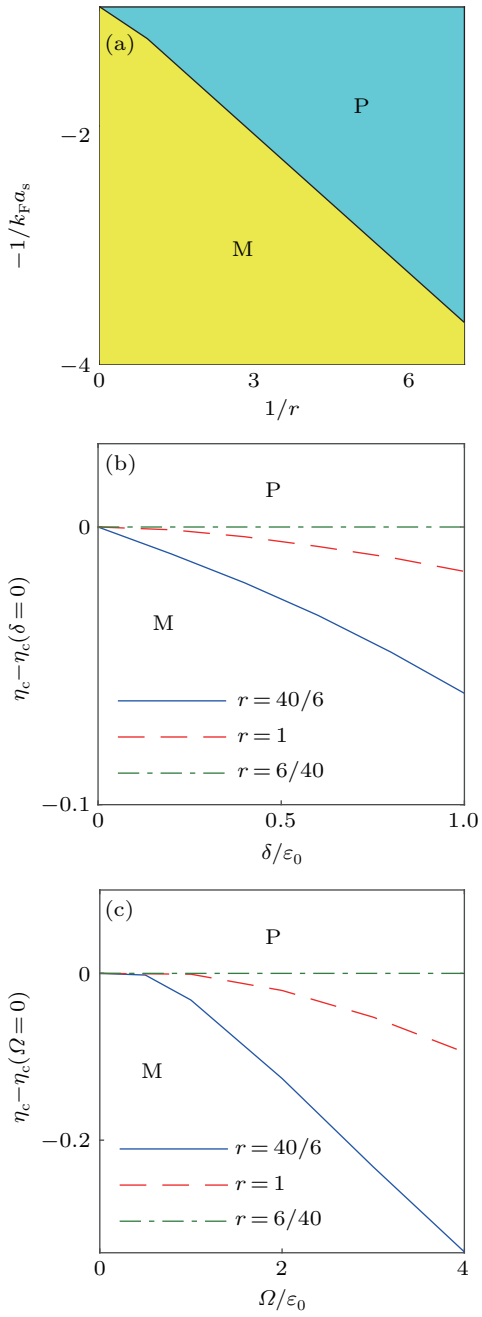

Fig. 6. (a) The evolution of the phase boundary in the $-(1/k_Fa_s)$–$1/r$ plane with $\Omega/\varepsilon_0=1$ and $\delta/\varepsilon_0=0.6$. (b) The critical interaction parameter η_c as a function of Zeeman field δ with $\Omega/\varepsilon_0=1$. (c) The critical interaction parameter η_c as a function of Raman coupling strength Ω with $\delta/\varepsilon_0=0.6$.

shown in Fig. 6(a), in general, the critical interaction parameter (a_s) of the polaron-to-molecule transition decreases with the inverse of the mass ratio $1/r$, suggesting that a light impurity is more favorable to form a polaron than a heavy one. In Figs. 6(b) and 6(c), we further investigate the transition point which is characterized by $\eta_c(x)-\eta_c(0)$ with $\eta\equiv-(1/k_Fa_s)$ as a function of $x=\delta$ or Ω for different mass ratios. It can be seen that the phase boundary of a heavy impurity is pushed into the BEC regime considerably with the increasing of δ or Ω (see the blue solid line of $r=40/6$), while a light impurity is not affected apparently by δ and Ω (referred to the green dash-dotted line of $r=6/40$). Note that for $\Omega=0$, the one-dimensional SOC can be gauged away and one gets the usual critical value of $-(1/k_Fa_s)\sim-3.65$ without SOC.

Compared to the previous work[61–64] where molecule states with a finite c.m. momentum are induced by the SOC, here in our case, the one-dimensional SOC of the impurity has more profound effect on the polaron state than the molecule state. When a high-dimensional SOC is introduced to the impurity atom, the enhanced single-particle ground-state degeneracy may also affect the molecule state strongly with unique features (For an impurity atom with two-dimensional Rashba-type SOC, the ring degeneracy of the single-particle state of the impurity may greatly enhance the pairing between the impurity and the atom in the Fermi sea with an unusual molecule state appearing even in a weak interaction regime), which nevertheless is out of the scope of the current work and we leave it for the future study.

In a summary, we theoretically investigate the properties of the polaron and molecular state of a spin–orbit coupled impurity in a three-dimensional Fermi gas. A couple of polaron and molecule states with finite c.m. momenta, which arises from the interplay between SOC and spin-selected interaction, are found to be the ground state. A discontinous transition between these polaron states is identified and manifested in the quasi-particle residue and effective mass of the polaron. Moreover, the polaron-to-molecule transition and the effects of a more general spin-dependent interaction and mass ratio are also discussed. These results pave a new way to study the interesting impurity physics brought by the SOC.

Appendix A: Derivation of the polaron state

We start from the variational wave-function of the polaron

$$|P\rangle=\sum_{\sigma}\phi_{\sigma}\hat{a}^{\dagger}_{\boldsymbol{Q}\sigma}|FS\rangle+\sum_{\boldsymbol{kq}\sigma}\phi_{\boldsymbol{kq}\sigma}\hat{a}^{\dagger}_{\boldsymbol{Q}+\boldsymbol{q}-\boldsymbol{k}\sigma}\hat{b}^{\dagger}_{\boldsymbol{k}}\hat{b}_{\boldsymbol{q}}|FS\rangle,\quad\text{(A1)}$$

where $\sigma=\uparrow/\downarrow$, ϕ_{σ} and $\phi_{\boldsymbol{kq}\sigma}$ are variational parameters. The summation is limited by $q<k_F$ and $k>k_F$. $|FS\rangle$ is the Fermi sea. The polaron variational wave function is normalized with $\langle P|P\rangle=\sum_{\sigma}|\phi_{\sigma}|^2+\sum_{\boldsymbol{kq}\sigma}|\phi_{\boldsymbol{kq}\sigma}|^2=1$. The variational energy of the polaron determined by $E_P=\langle P|\hat{H}|P\rangle$ is derived as

$$\begin{aligned}
&\sum_{\sigma}\frac{\boldsymbol{Q}^2+\boldsymbol{k}_0^2}{2m_a}|\phi_{\sigma}|^2+\left(\frac{\boldsymbol{k}_0\cdot\boldsymbol{Q}}{m_a}+\frac{\delta}{2}\right)\left(|\phi_{\uparrow}|^2-|\phi_{\downarrow}|^2\right)\\
&+\sum_{\boldsymbol{kq}\sigma}\frac{|\boldsymbol{Q}+\boldsymbol{k}-\boldsymbol{q}|^2+\boldsymbol{k}_0^2}{2m_a}|\phi_{\boldsymbol{kq}\sigma}|^2\\
&+\sum_{\boldsymbol{kq}}\left(\frac{\boldsymbol{k}_0\cdot(\boldsymbol{Q}+\boldsymbol{k}-\boldsymbol{q})}{m_a}+\frac{\delta}{2}\right)\left(|\phi_{\boldsymbol{kq}\uparrow}|^2-|\phi_{\boldsymbol{kq}\downarrow}|^2\right)\\
&+\sum_{\boldsymbol{kq}}\left(\frac{\boldsymbol{k}^2}{2m_b}-\frac{\boldsymbol{q}^2}{2m_b}\right)|\phi_{\boldsymbol{kq}\sigma}|^2\\
&+\frac{g_{\uparrow}}{V}\left[\sum_{\boldsymbol{q}}|\phi_{\uparrow}|^2+\sum_{\boldsymbol{kk'q}}\phi^{*}_{\boldsymbol{kq}\uparrow}\phi_{\boldsymbol{k'q}\uparrow}+\sum_{\boldsymbol{kq}}\left(\phi^{*}_{\uparrow}\phi_{\boldsymbol{kq}\uparrow}+\phi_{\uparrow}\phi^{*}_{\boldsymbol{kq}\uparrow}\right)\right]
\end{aligned}$$

$$+\frac{g_\downarrow}{V}\left[\sum_{\boldsymbol{q}}|\phi_\downarrow|^2+\sum_{\boldsymbol{k}\boldsymbol{k}'\boldsymbol{q}}\phi^*_{\boldsymbol{k}\boldsymbol{q}\downarrow}\phi_{\boldsymbol{k}'\boldsymbol{q}\downarrow}+\sum_{\boldsymbol{k}\boldsymbol{q}}\left(\phi^*_\downarrow\phi_{\boldsymbol{k}\boldsymbol{q}\downarrow}+\phi_\downarrow\phi^*_{\boldsymbol{k}\boldsymbol{q}\downarrow}\right)\right]$$
$$+\frac{\Omega}{2}\left(\phi^*_\uparrow\phi_\downarrow+\text{h.c.}\right)+\frac{\Omega}{2}\sum_{\boldsymbol{k}\boldsymbol{q}}\left(\phi^*_{\boldsymbol{k}\boldsymbol{q}\uparrow}\phi_{\boldsymbol{k}\boldsymbol{q}\downarrow}+\text{h.c.}\right)$$
$$=E_{\text{P}}\left(\sum_{\boldsymbol{k}\sigma}|\phi_\sigma|^2+\sum_{\boldsymbol{k}\boldsymbol{q}\sigma}|\phi_{\boldsymbol{k}\boldsymbol{q}\sigma}|^2\right). \tag{A2}$$

By variational minimizing the energy functional $\langle P|E_{\text{P}}-\hat{H}|P\rangle$, we obtain the following set of equations:

$$\left(E_{\text{P}}-\varepsilon_\downarrow+\frac{\delta}{2}\right)\phi_\downarrow-\frac{g_\downarrow}{V}\left(\sum_{\boldsymbol{q}}\phi_\downarrow+\sum_{\boldsymbol{k}\boldsymbol{q}}\phi_{\boldsymbol{k}\boldsymbol{q}\downarrow}\right)=\frac{\Omega}{2}\phi_\uparrow, \tag{A3}$$

$$\left(E_{\text{P}}-\varepsilon_\uparrow-\frac{\delta}{2}\right)\phi_\uparrow-\frac{g_\uparrow}{V}\left(\sum_{\boldsymbol{q}}\phi_\uparrow+\sum_{\boldsymbol{k}\boldsymbol{q}}\phi_{\boldsymbol{k}\boldsymbol{q}\uparrow}\right)=\frac{\Omega}{2}\phi_\downarrow, \tag{A4}$$

$$\left(E_{\text{P}}-\varepsilon_{\boldsymbol{k}\boldsymbol{q}\downarrow}+\frac{\delta}{2}\right)\phi_{\boldsymbol{k}\boldsymbol{q}\downarrow}-\frac{g_\downarrow}{V}\left(\phi_\downarrow+\sum_{\boldsymbol{k}'}\phi_{\boldsymbol{k}'\boldsymbol{q}\downarrow}\right)=\frac{\Omega}{2}\phi_{\boldsymbol{k}\boldsymbol{q}\uparrow}, \tag{A5}$$

$$\left(E_{\text{P}}-\varepsilon_{\boldsymbol{k}\boldsymbol{q}\uparrow}-\frac{\delta}{2}\right)\phi_{\boldsymbol{k}\boldsymbol{q}\uparrow}-\frac{g_\uparrow}{V}\left(\phi_\uparrow+\sum_{\boldsymbol{k}'}\phi_{\boldsymbol{k}'\boldsymbol{q}\uparrow}\right)=\frac{\Omega}{2}\phi_{\boldsymbol{k}\boldsymbol{q}\downarrow}. \tag{A6}$$

From Eqs. (A3) and (A4), we obtain

$$\sum_{\boldsymbol{k}'}\phi_{\boldsymbol{k}'\boldsymbol{q}\uparrow}=\frac{g_\uparrow}{V}A_{\boldsymbol{q}\uparrow}\left(\phi_\uparrow+\sum_{\boldsymbol{k}'}\phi_{\boldsymbol{k}'\boldsymbol{q}\uparrow}\right)+\frac{g_\downarrow\Omega}{2V}A_{\boldsymbol{q}}\left(\phi_\downarrow+\sum_{\boldsymbol{k}'}\phi_{\boldsymbol{k}'\boldsymbol{q}\downarrow}\right), \tag{A7}$$

$$\sum_{\boldsymbol{k}'}\phi_{\boldsymbol{k}'\boldsymbol{q}\downarrow}=\frac{g_\downarrow}{V}A_{\boldsymbol{q}\downarrow}\left(\phi_\downarrow+\sum_{\boldsymbol{k}'}\phi_{\boldsymbol{k}'\boldsymbol{q}\downarrow}\right)+\frac{g_\uparrow\Omega}{2V}A_{\boldsymbol{q}}\left(\phi_\uparrow+\sum_{\boldsymbol{k}'}\phi_{\boldsymbol{k}'\boldsymbol{q}\uparrow}\right), \tag{A8}$$

where

$$A_{\boldsymbol{q}\uparrow}\equiv\sum_{\boldsymbol{k}}\left[\left(E_{\text{P}}-\varepsilon_{\boldsymbol{k}\boldsymbol{q}\uparrow}-\frac{\delta}{2}\right)-\frac{\Omega^2}{4}\left(E_{\text{P}}-\varepsilon_{\boldsymbol{k}\boldsymbol{q}\downarrow}+\frac{\delta}{2}\right)^{-1}\right]^{-1},$$

$$A_{\boldsymbol{q}\downarrow}\equiv\sum_{\boldsymbol{k}}\left[\left(E_{\text{P}}-\varepsilon_{\boldsymbol{k}\boldsymbol{q}\downarrow}-\frac{\delta}{2}\right)-\frac{\Omega^2}{4}\left(E_{\text{P}}-\varepsilon_{\boldsymbol{k}\boldsymbol{q}\uparrow}+\frac{\delta}{2}\right)^{-1}\right]^{-1},$$

$$A_{\boldsymbol{q}}\equiv\sum_{\boldsymbol{k}}\left[\left(E_{\text{P}}-\varepsilon_{\boldsymbol{k}\boldsymbol{q}\downarrow}+\frac{\delta}{2}\right)\left(E_{\text{P}}-\varepsilon_{\boldsymbol{k}\boldsymbol{q}\uparrow}-\frac{\delta}{2}\right)-\frac{\Omega^2}{4}\right]^{-1}.$$

Substituting Eqs. (A7) and (A8) into Eqs. (A5) and (A6), we get

$$\sum_{\boldsymbol{q}}\phi_\uparrow+\sum_{\boldsymbol{k}\boldsymbol{q}}\phi_{\boldsymbol{k}\boldsymbol{q}\uparrow}=\sum_{\boldsymbol{q}}\frac{\left(1-\frac{g_\downarrow}{V}A_{\boldsymbol{q}\downarrow}\right)\phi_\uparrow+\frac{g_\downarrow\Omega}{2V}\phi_\downarrow}{\left(1-\frac{g_\downarrow}{V}A_{\boldsymbol{q}\downarrow}\right)\left(1-\frac{g_\uparrow}{V}A_{\boldsymbol{q}\uparrow}\right)-\frac{g_\downarrow g_\uparrow\Omega^2}{4V}A^2_{\boldsymbol{q}}}, \tag{A9}$$

$$\sum_{\boldsymbol{q}}\phi_\downarrow+\sum_{\boldsymbol{k}\boldsymbol{q}}\phi_{\boldsymbol{k}\boldsymbol{q}\downarrow}=\sum_{\boldsymbol{q}}\frac{\left(1-\frac{g_\uparrow}{V}A_{\boldsymbol{q}\uparrow}\right)\phi_\downarrow+\frac{g_\uparrow\Omega}{2V}\phi_\uparrow}{\left(1-\frac{g_\uparrow}{V}A_{\boldsymbol{q}\uparrow}\right)\left(1-\frac{g_\downarrow}{V}A_{\boldsymbol{q}\downarrow}\right)-\frac{g_\uparrow g_\downarrow\Omega^2}{4V}A^2_{\boldsymbol{q}}}. \tag{A10}$$

From Eqs. (A9) and (A10), we find

$$\left[\left(E_{\text{P}}-\varepsilon_\downarrow+\frac{\delta}{2}\right)-\frac{g_\downarrow}{V}\sum_{\boldsymbol{q}}\frac{1-\frac{g_\uparrow}{V}A_{\boldsymbol{q}\uparrow}}{\left(1-\frac{g_\uparrow}{V}A_{\boldsymbol{q}\uparrow}\right)\left(1-\frac{g_\downarrow}{V}A_{\boldsymbol{q}\downarrow}\right)-\frac{g_\uparrow g_\downarrow\Omega^2}{4V}A^2_{\boldsymbol{q}}}\right]\phi_\uparrow$$
$$-\frac{\Omega}{2}\left(1-\frac{g_\uparrow g_\downarrow}{V^2}\sum_{\boldsymbol{q}}\frac{1}{\left(1-\frac{g_\uparrow}{V}A_{\boldsymbol{q}\uparrow}\right)\left(1-\frac{g_\downarrow}{V}A_{\boldsymbol{q}\downarrow}\right)-\frac{g_\uparrow g_\downarrow\Omega^2}{4V}A^2_{\boldsymbol{q}}}\right)\phi_\downarrow=0, \tag{A11}$$

$$\left[\left(E_{\text{P}}-\varepsilon_\uparrow-\frac{\delta}{2}\right)-\frac{g_\uparrow}{V}\sum_{\boldsymbol{q}}\frac{1-\frac{g_\downarrow}{V}A_{\boldsymbol{q}\downarrow}}{\left(1-\frac{g_\uparrow}{V}A_{\boldsymbol{q}\uparrow}\right)\left(1-\frac{g_\downarrow}{V}A_{\boldsymbol{q}\downarrow}\right)-\frac{g_\uparrow g_\downarrow\Omega^2}{4V}A^2_{\boldsymbol{q}}}\right]\phi_\downarrow$$
$$-\frac{\Omega}{2}\left(1-\frac{g_\uparrow g_\downarrow}{V^2}\sum_{\boldsymbol{q}}\frac{1}{\left(1-\frac{g_\uparrow}{V}A_{\boldsymbol{q}\uparrow}\right)\left(1-\frac{g_\downarrow}{V}A_{\boldsymbol{q}\downarrow}\right)-\frac{g_\uparrow g_\downarrow\Omega^2}{4V}A^2_{\boldsymbol{q}}}\right)\phi_\uparrow=0. \tag{A12}$$

Finally, we get the equation of the poalron energy E_{P},

$$\left[\left(E_{\text{P}}-\varepsilon_\downarrow+\frac{\delta}{2}\right)-\frac{g_\downarrow}{V}\sum_{\boldsymbol{q}}\frac{1-\frac{g_\uparrow}{V}A_{\boldsymbol{q}\uparrow}}{\left(1-\frac{g_\uparrow}{V}A_{\boldsymbol{q}\uparrow}\right)\left(1-\frac{g_\downarrow}{V}A_{\boldsymbol{q}\downarrow}\right)-\frac{g_\uparrow g_\downarrow\Omega^2}{4V}A^2_{\boldsymbol{q}}}\right]$$

$$\times\left[\left(E_{\rm P}-\varepsilon_{\uparrow}-\frac{\delta}{2}\right)-\frac{g_{\uparrow}}{V}\sum_{q}\frac{1-\frac{g_{\downarrow}}{V}A_{q\downarrow}}{\left(1-\frac{g_{\uparrow}}{V}A_{q\uparrow}\right)\left(1-\frac{g_{\downarrow}}{V}A_{q\downarrow}\right)-\frac{g_{\uparrow}g_{\downarrow}\Omega^2}{4V}A_q^2}\right]$$

$$-\frac{\Omega^2}{4}\left(1-\frac{g_{\uparrow}g_{\downarrow}}{V^2}\sum_{q}\frac{1}{\left(1-\frac{g_{\uparrow}}{V}A_{q\uparrow}\right)\left(1-\frac{g_{\downarrow}}{V}A_{q\downarrow}\right)-\frac{g_{\uparrow}g_{\downarrow}\Omega^2}{4V}A_q^2}\right)^2=0. \tag{A13}$$

For $g_{\downarrow}=0$, we recover the energy Eq. (4) in the maintext.

Appendix B: Quasiparticle residue of the polaron state

The total quasiparticle residue $Z=Z_{\uparrow}+Z_{\downarrow}$ comprised of the contributions of different spin states with $Z_{\uparrow}=|\phi_{\uparrow}|^2$ and $Z_{\downarrow}=|\phi_{\downarrow}|^2$. Here we focus on the case of $g_{\downarrow}=0$. From Eq. (A7), we have $Z_{\downarrow}=(\Omega^2/4)(E_{\rm P}-\varepsilon_{\downarrow}+\delta/2)^{-2}Z_{\uparrow}$. And the normalization condition becomes

$$\left[1+\frac{\Omega^2}{4}\left(E_{\rm P}-\varepsilon_{\downarrow}+\frac{\delta}{2}\right)^{-2}\right]Z_{\uparrow}$$
$$+\sum_{kq\sigma}\left[1+\frac{\Omega^2}{4}\left(E_{\rm P}-\varepsilon_{kq\downarrow}+\frac{\delta}{2}\right)^{-2}\right]|\phi_{kq\uparrow}|^2=1. \tag{B1}$$

Substituting Eq. (A11) into Eq. (A10), we have

$$\left[\left(E_{\rm P}-\varepsilon_{kq\uparrow}-\frac{\delta}{2}\right)-\frac{\Omega^2}{4}\left(E_{\rm P}-\varepsilon_{kq\downarrow}+\frac{\delta}{2}\right)^{-1}\right]^2|\phi_{kq\uparrow}|^2$$
$$=\frac{g^2}{V^2}\left\{1-\frac{g}{V}\sum_{k}\left[\left(E_{\rm P}-\varepsilon_{kq\uparrow}-\frac{\delta}{2}\right)\right.\right.$$
$$\left.\left.-\frac{\Omega^2}{4}\left(E_{\rm P}-\varepsilon_{kq\downarrow}+\frac{\delta}{2}\right)^{-1}\right]^{-1}\right\}^{-2}Z_{\uparrow}. \tag{B2}$$

Taking use of Eq. (B1), we obtain $Z_{\uparrow}$

$$1=\left[1+\frac{\Omega^2}{4}\left(E_{\rm P}-\varepsilon_{\downarrow}+\frac{\delta}{2}\right)^{-2}\right]Z_{\uparrow}$$
$$+\sum_{kq\sigma}\left[1+\frac{\Omega^2}{4}\left(E_{\rm P}-\varepsilon_{kq\downarrow}+\frac{\delta}{2}\right)^{-2}\right]$$
$$\times\left[\left(E_{\rm P}-\varepsilon_{kq\uparrow}-\frac{\delta}{2}\right)-\frac{\Omega^2}{4}\left(E_{\rm P}-\varepsilon_{kq\downarrow}+\frac{\delta}{2}\right)^{-1}\right]^{-2}$$
$$\times\frac{g^2}{V^2}\left\{1-\frac{g}{V}\sum_{k}\left[\left(E_{\rm P}-\varepsilon_{kq\uparrow}-\frac{\delta}{2}\right)\right.\right.$$
$$\left.\left.-\frac{\Omega^2}{4}\left(E_{\rm P}-\varepsilon_{kq\downarrow}+\frac{\delta}{2}\right)^{-1}\right]^{-1}\right\}^{-2}Z_{\uparrow}. \tag{B3}$$

Finally, we get the inverse of $Z_{\uparrow}$

$$\frac{1}{Z_{\uparrow}}=1+\frac{\Omega^2}{4}\left(E_{\rm P}-\varepsilon_{\downarrow}+\frac{\delta}{2}\right)^{-2}$$
$$+\sum_{kq\sigma}\left[1+\frac{\Omega^2}{4}\left(E_{\rm P}-\varepsilon_{kq\downarrow}+\frac{\delta}{2}\right)^{-2}\right]$$
$$\times\left[\left(E_{\rm P}-\varepsilon_{kq\uparrow}-\frac{\delta}{2}\right)-\frac{\Omega^2}{4}\left(E_{\rm P}-\varepsilon_{kq\downarrow}+\frac{\delta}{2}\right)^{-1}\right]^{-2}$$
$$\times\left\{1-\frac{g}{V}\sum_{k}\left[\left(E_{\rm P}-\varepsilon_{kq\uparrow}-\frac{\delta}{2}\right)\right.\right.$$
$$\left.\left.-\frac{\Omega^2}{4}\left(E_{\rm P}-\varepsilon_{kq\downarrow}+\frac{\delta}{2}\right)^{-1}\right]^{-1}\right\}^{-2}. \tag{B4}$$

Appendix C: Derivation of the molecular state

With the molecule state variational wave-function $|M\rangle$ in Eq. (8) of the maintext, the molecule state energy $E_{\rm M}$ (relative to the Fermi sea) satisfies

$$E_{\rm M}=\sum_{k\sigma}\left(\frac{|q-k|^2}{2m_{\rm a}}+\frac{k_0^2}{2m_{\rm a}}+\frac{k^2}{2m_{\rm b}}\right)|\psi_{k\sigma}|^2$$
$$+\sum_{k}\left[\frac{(q-k)\cdot k_0}{m_{\rm a}}+\frac{\delta}{2}\right]\left(|\psi_{k\uparrow}|^2-|\psi_{k\downarrow}|^2\right)$$
$$+\frac{\Omega}{2}\sum_{k}(\psi_{k\uparrow}^{*}\psi_{k\downarrow}+{\rm c.c.})+\sum_{kk'\sigma}\frac{g_{\sigma}}{V}\psi_{k\sigma}^{*}\psi_{k'\sigma}. \tag{C1}$$

Minimizing the energy functional $\langle M|\hat{H}|M\rangle$, we obtain the following equations:

$$\varepsilon_{k\uparrow}\psi_{k\uparrow}+\frac{\Omega}{2}\psi_{k\downarrow}+\frac{g_{\uparrow}}{V}\sum_{k}\psi_{k'\uparrow}=(E_{\rm M}+E_{\rm F})\psi_{k\uparrow}, \tag{C2}$$

$$\varepsilon_{k\downarrow}\psi_{k\downarrow}+\frac{\Omega}{2}\psi_{k\uparrow}+\frac{g_{\downarrow}}{V}\sum_{k}\psi_{k'\downarrow}=(E_{\rm M}+E_{\rm F})\psi_{k\downarrow}, \tag{C3}$$

where

$$\varepsilon_{k\uparrow}=\frac{|q+k+k_0|^2}{2m_{\rm a}}+\frac{k^2}{2m_{\rm b}}+\frac{\delta}{2},$$
$$\varepsilon_{k\downarrow}=\frac{|q+k-k_0|^2}{2m_{\rm a}}+\frac{k^2}{2m_{\rm b}}-\frac{\delta}{2}.$$

From Eqs. (C2) and (C3), we obtain

$$\eta_k\psi_{k\uparrow}=\frac{g_{\uparrow}}{V}(E_{\rm M}+E_{\rm F}-\varepsilon_{k\downarrow})\sum_{k'}\psi_{k'\uparrow}+\frac{g_{\downarrow}\Omega}{2V}\sum_{k'}\psi_{k'\downarrow}, \tag{C4}$$

$$\eta_k\psi_{k\downarrow}=\frac{g_{\downarrow}}{V}(E_{\rm M}+E_{\rm F}-\varepsilon_{k\uparrow})\sum_{k'}\psi_{k'\downarrow}+\frac{g_{\uparrow}\Omega}{2V}\sum_{k'}\psi_{k'\uparrow}. \tag{C5}$$

where $\eta_{\boldsymbol{k}} = (E_{\rm M}+E_{\rm F}-\varepsilon_{\boldsymbol{k}\downarrow})(E_{\rm M}+E_{\rm F}-\varepsilon_{\boldsymbol{k}\uparrow})-\Omega^2/4$. From Eqs. (C4) and (C5), we get

$$\left(1-\frac{g_\uparrow}{V}\sum_{\boldsymbol{k}}\eta_{\boldsymbol{k}}^{-1}\left(E_{\rm M}+E_{\rm F}-\varepsilon_{\boldsymbol{k}\downarrow}\right)\right)\sum_{\boldsymbol{k}'}\psi_{\boldsymbol{k}'\uparrow} -\frac{g_\downarrow\Omega}{2V}\sum_{\boldsymbol{k}}\eta_{\boldsymbol{k}}^{-1}\sum_{\boldsymbol{k}'}\psi_{\boldsymbol{k}'\downarrow}=0, \tag{C6}$$

$$\left(1-\frac{g_\downarrow}{V}\sum_{\boldsymbol{k}}\eta_{\boldsymbol{k}}^{-1}\left(E_{\rm M}+E_{\rm F}-\varepsilon_{\boldsymbol{k}\uparrow}\right)\right)\sum_{\boldsymbol{k}'}\psi_{\boldsymbol{k}'\downarrow} -\frac{g_\uparrow\Omega}{2V}\sum_{\boldsymbol{k}}\eta_{\boldsymbol{k}}^{-1}\sum_{\boldsymbol{k}'}\psi_{\boldsymbol{k}'\uparrow}=0. \tag{C7}$$

Finally, the self-consistent equation of the molecule energy is

$$\left(1-\frac{g_\uparrow}{V}\sum_{\boldsymbol{k}}\eta_{\boldsymbol{k}}^{-1}(E_{\rm M}+E_{\rm F}-\varepsilon_{\boldsymbol{k}\downarrow})\right) \times\left(1-\frac{g_\downarrow}{V}\sum_{\boldsymbol{k}}\eta_{\boldsymbol{k}}^{-1}(E_{\rm M}+E_{\rm F}-\varepsilon_{\boldsymbol{k}\uparrow})\right) -\frac{g_\uparrow g_\downarrow\Omega^2}{4V}\left(\sum_{\boldsymbol{k}}\eta_{\boldsymbol{k}}^{-1}\right)^2=0. \tag{C8}$$

Similarly, we go back to Eq. (9) in the maintext for $g_\downarrow=0$.

Next, we calculate $\psi_{\boldsymbol{k}\sigma}$ for $g_\downarrow=0$. From Eq. (C4), we obtain

$$\left[\varepsilon_{\boldsymbol{k}\uparrow}-\frac{\Omega^2}{4}\varepsilon_{\boldsymbol{k}\downarrow}^{-1}\right]\psi_{\boldsymbol{k}\uparrow}=\left[\varepsilon_{\boldsymbol{k}'\uparrow}-\frac{\Omega^2}{4}\varepsilon_{\boldsymbol{k}'\downarrow}^{-1}\right]\psi_{\boldsymbol{k}'\uparrow}. \tag{C9}$$

Then, we have

$$\psi_{\boldsymbol{k}\uparrow}=\frac{1}{\sqrt{A}}\left[\varepsilon_{\boldsymbol{k}\uparrow}-\frac{\Omega^2}{4}\varepsilon_{\boldsymbol{k}\downarrow}^{-1}\right]^{-1}, \tag{C10}$$

$$\psi_{\boldsymbol{k}\downarrow}=\frac{1}{\sqrt{A}}\frac{\Omega}{2}\varepsilon_{\boldsymbol{k}\downarrow}^{-1}\left[\varepsilon_{\boldsymbol{k}\uparrow}-\frac{\Omega^2}{4}\varepsilon_{\boldsymbol{k}\downarrow}^{-1}\right]^{-1}, \tag{C11}$$

where

$$A=\sum_{\boldsymbol{k}}\left(1+\frac{\Omega^2}{4}\varepsilon_{\boldsymbol{k}\downarrow}^{-2}\right)\left[\varepsilon_{\boldsymbol{k}\uparrow}-\frac{\Omega^2}{4}\varepsilon_{\boldsymbol{k}\downarrow}^{-1}\right]^{-2}. \tag{C12}$$

References

[1] Kondo J 1964 *Prog. Theor. Phys.* **32** 37
[2] Anderson P W 1967 *Phys. Rev. Lett.* **18** 1049
[3] Mannella N, Yang W L, Zhou X J, Zheng H, Mitchell J F, Zaanen J, Devereaux T P, Nagaosa N, Hussain Z and Shen Z 2005 *Nature* **438** 474
[4] Devreese J T and Alexandrov A S 2009 *Rep. Prog. Phys.* **72** 066501
[5] Ospelkaus, Ospelkaus S C, Wille O, Succo M, Ernst P, Sengstock K and Bongs K 2006 *Phys. Rev. Lett.* **96** 180403
[6] Buonsante P, Massel F, Penna V and Vezzani A 2009 *Phys. Rev. A* **79** 013623
[7] Zhang X, Wen Y and Eggert S 2010 *Phys. Rev. B* **82** 220501(R)
[8] Privitera A and Hofstetter W 2010 *Phys. Rev. A* **82** 063614
[9] Jiang L, Baksmaty L O, Hu H, Chen Y and Pu H 2011 *Phys. Rev. A* **83** 061604(R)
[10] Spethmann N, Kindermann F, John S, Weber C, Meschede D and Widera A 2012 *Phys. Rev. Lett.* **109** 235301
[11] Knap M, Shashi A, Nishida Y, Imambekov A, Abanin D A and Demler E 2012 *Phys. Rev. X* **2** 041020
[12] Hu H, Jiang L, Pu H, Chen Y and Liu X 2013 *Phys. Rev. Lett.* **110** 020401
[13] Zwierlein M W, Schirotzek A, Schunck C H and Ketterle W 2006 *Science* **311** 492
[14] Partridge G B, Li W, Kamar R I, Liao Y and Hulet R G 2006 *Science* **311** 503
[15] Shin Y, Zwierlein M W, Schunck C H, Schirotzek A and Ketterle W 2006 *Phys. Rev. Lett.* **97** 030401
[16] Chevy F 2006 *Phys. Rev. A* **74** 063628
[17] Combescot R, Recati A, Lobo C and Chevy F 2007 *Phys. Rev. Lett.* **98** 180402
[18] Prokof'ev N and Svistunov B 2008 *Phys. Rev. B* **77** 020408
[19] Schirotzek A, Wu C, Sommer A and Zwierlein M W 2009 *Phys. Rev. Lett.* **102** 230402
[20] Koschorreck M, Pertot D, Vogt E, Fröhlich B, Feld M and Köhl M 2012 *Nature* **485** 619
[21] Nascimbene S, Navon N, Jiang K J, Tarruell L, Teichmann M, McKeever J, Chevy F and Salomon C 2009 *Phys. Rev. Lett.* **103** 170402
[22] Punk M, Dumitrescu P T and Zwerger W 2009 *Phys. Rev. A* **80** 053605
[23] Bruun G M and Massignan P 2010 *Phys. Rev. Lett.* **105** 020403
[24] Chevy F and Mora C 2010 *Rep. Prog. Phys.* **73** 112401
[25] Zöllner S, Bruun G M and Pethick C J 2011 *Phys. Rev. A* **83** 021603(R)
[26] Parish M M 2011 *Phys. Rev. A* **83** 051603(R)
[27] Ngampruetikorn V, Levinsen J and Parish M M 2012 *Europhys. Lett.* **98** 30005
[28] Qi R and Zhai H 2012 *Phys. Rev. A* **85** 041603(R)
[29] Vlietinck J, Ryckebusch J and Van Houcke K 2013 *Phys. Rev. B* **87** 115133
[30] Massignan P, Zaccanti M and Bruun G M 2014 *Rep. Prog. Phys.* **77** 034401
[31] Yi W and Cui X 2015 *Phys. Rev. A* **92** 013620
[32] Hu H, Mulkerin B C, Wang J, and Liu X 2018 *Phys. Rev. A* **98** 013626
[33] Oppong N D, Riegger L, Bettermann O, Hfer M, Levinsen J, Parish M M, Bloch I and Flling S 2019 *Phys. Rev. Lett.* **122** 193604
[34] Van Houcke K, Werner F and Rossi R 2020 *Phys. Rev. B* **101** 045134
[35] Julià-Farré S, Mller M, Lewenstein M and Dauphin A 2020 *Phys. Rev. Lett.* **125** 240601
[36] Hu M G, Van de Graaff J M, Kedar D, Corson J P, Cornell E A and Jin D S 2016 *Phys. Rev. Lett.* **117** 055301
[37] Guenther N, Massignan P, Lewenstein M and Bruun G M 2018 *Phys. Rev. Lett.* **120** 050405
[38] Field B, Levinsen J and Parish M M 2020 *Phys. Rev. Lett.* **101** 013623
[39] Hryhorchak O, Panochko G and Pastukhov V 2020 *Phys. Lett. A* **384** 126934
[40] Massignan P, Yegovtsev N and Gurarie V 2021 *Phys. Rev. Lett.* **126** 123403
[41] Trefzger C and Castin Y 2012 *Phys. Rev. A* **85** 053612
[42] Parish M M and Levinsen J 2013 *Phys. Rev. A* **87** 033616
[43] Ma Y and Cui X 2019 *Phys. Rev. A* **100** 062712
[44] Cui X 2020 *Phys. Rev. A* **102** 061301(R)
[45] Chin C, Grimm R, Julienne P and Tiesinga T 2010 *Rev. Mod. Phys.* **82** 1225
[46] Lin Y J, Jimeńez-Garcá K and Spielman I B 2011 *Nature* **471** 83
[47] Wang P J, Yu Z Q, Fu Z, Miao J, Huang L, Chai S, Zhai H and Zhang J 2012 *Phys. Rev. Lett.* **109** 095301
[48] Cheuk L W, Sommer A T, Hadzibabic Z, Yefsah T, Bakr W S and Zwierlein M W 2012 *Phys. Rev. Lett.* **109** 095302
[49] Galitski V and Spielman I B 2013 *Nature* **494** 49
[50] Wu Z, Zhang L, Sun W, Xu X, Wang B, Ji S, Deng Y, Chen S, Liu X J and Pan J W 2016 *Science* **354** 83
[51] Wang C, Gao C, Jian C and Zhai H 2010 *Phys. Rev. Lett.* **105** 160403
[52] Campbell D L, Juzelinas G and Spielman I B 2011 *Phys. Rev. A* **84** 025602
[53] Zhang J, Ji S, Chen Z, Zhang L, Du Z, Yan B, Pan G, Zhao B, Deng Y, Zhai H, Chen S and Pan J 2012 *Phys. Rev. Lett.* **109** 115301
[54] Goldman N, Juzeliunas G, Öhberg P and Spielman I B 2014 *Rep. Prog. Phys.* **77** 126401
[55] Zhai H 2015 *Rep. Prog. Phys.* **78** 026001
[56] Xu Y, Zhang F and Zhang C 2015 *Phys. Rev. Lett.* **115** 265304

[57] Livi L F, Cappellini G, Diem M, Franchi L, Clivati C, Frittelli M, Levi F, Calonico D, Catani J, Inguscio M and Fallani L 2016 *Phys. Rev. Lett.* **117** 220401

[58] Shteynas B, Lee J, Top F, Li R, Jamison A O, Juzeliūnas G and Ketterle W 2019 *Phys. Rev. Lett.* **123** 033203

[59] Shi T, Wang L, Wang J and Zhang W 2020 *Acta Phys. Sin.* **69** 016701 (in Chinese)

[60] Cui X and Zhou Q 2013 *Phys. Rev. A* **87** 031604(R)

[61] Yi W and Zhang W 2012 *Phys. Rev. Lett.* **109** 140402

[62] Zhou L, Cui X and Yi W 2014 *Phys. Rev. Lett.* **112** 195301

[63] Qiu X, Cui X and Yi W 2016 *Phys. Rev. A* **94** 051604(R)

[64] Shi Y, Lu Z, Wang J and Zhang W 2019 *Acta Phys. Sin.* **68** 040305 (in Chinese)

[65] Randeria M, Duan J and Shieh L 1989 *Phys. Rev. Lett.* **62** 981